Computer Communications 35 (2012) 1494–1506

Contents lists available at SciVerse ScienceDirect

Computer Communications

journal homepage: www.elsevier.com/locate/comcom

The viral conductance of a network

Piet Van Mieghem *

Delft University of Technology, Faculty of Electrical Engineering, Mathematics and Computer Science, P.O. Box 5031, 2600 GA Delft, The Netherlands

ARTICLE INFO

Article history:
Received 9 April 2012
Received in revised form 15 April 2012
Accepted 18 April 2012
Available online 2 May 2012

Keywords:
SIS epidemics
Network robustness
Viral conductance
Epidemic threshold

ABSTRACT

Besides the epidemic threshold, the recently proposed viral conductance ψ by Kooij et al. [11] may be regarded as an additional characterizer of the viral robustness of a network, that measures the overall ease in which viruses can spread in a particular network. Motivated to explain observed features of the viral conductance ψ in simulations [29], we have analysed this metric in depth using the N-intertwined SIS epidemic model, that upper bounds the real infection probability in any network and, hence, provides safe-side bounds on which network protection can be based. Our study here derives a few exact results for ψ, a number of different lower and upper bounds for ψ with variable accuracy. We also extend the theory of the N-intertwined SIS epidemic model, by deducing formal series expansions of the steady-state fraction of infected nodes for any graph and any effective infection rate, that result in a series for the viral conductance ψ. Though approximate, we illustrate here that the N-intertwined SIS epidemic model is so far the only SIS model *on networks* that is analytically tractable, and valuable to provide first order estimates of the epidemic impact in networks. Finally, inspired by the analogy between virus spread and synchronization of coupled oscillators in a network, we propose the synchronizability as the analogue of the viral conductance.

1. Introduction

We investigate the influence of the network topology on the spread of viruses, digital as well as biological ones, whose dynamics is modeled by a susceptible-infected-susceptible (SIS) type of process [2]. Digital viruses (of all kind, and generally called malware) are living in cyberspace and use mainly the Internet as the transport media, while biological viruses contaminate other living beings on earth and use "contacts" among their victims as their propagation networks. The increasing threats from cybercrime and the expected outbreak of new lethal, biological viruses justify studies on virus spread in graphs. In particular, network operators are interested to know (a) how vulnerable their network is for epidemics and (b) how to protect or modify their infrastructure, most often, at minimal cost (see e.g. [10]). In contrast to the negative connotation of a threat, information spread (news, rumors, etc.) in the new types of on-line social networks like Facebook, Twitter, Digg [20], etc. resembles epidemic diffusion. While this analogy still needs to be verified and evaluated via extensive measurements, epidemic theory is expected to be fruitful in assessing the spreading speed and depth (i.e. how many users are reached) of news in social networks.

A network is represented by an undirected graph $G(N, L)$ with N nodes and L links. The network topology is described by a symmetric adjacency matrix A, in which the element $a_{ij} = a_{ji} = 1$ if there is a link between nodes i and j, otherwise $a_{ij} = 0$. In the sequel, we confine ourselves and make the following simplifying assumptions. The state of a node i is specified by a Bernoulli random variable $X_i \in \{0, 1\}$: $X_i = 0$ for a healthy node and $X_i = 1$ for an infected node. A node i at time t can be in one of the two states: *infected*, with probability $v_i(t) = \Pr[X_i(t) = 1]$ or *healthy*, with probability $1 - v_i(t)$. We assume that the curing process per node i is a Poisson process with rate δ, and that the infection rate per link is a Poisson process with rate β. All involved Poisson processes are independent. The effective infection rate is defined as $\tau = \frac{\beta}{\delta}$. This is the general description of the simplest type of a SIS virus spread model in a network and the challenge is to determine the virus infection probability $v_i(t)$ for each node i in the graph G. This SIS model can be expressed exactly in terms of a continuous-time Markov model with 2^N states as shown in [27]. Unfortunately, the exponentially increasing state space with N prevents the determination of the set of $\{v_i(t)\}_{1 \leqslant i \leqslant N}$ in realistic networks, which has triggered a spur of research to find good approximate solutions. For an overview of SIS heuristics and numerous extensions, we refer to [3,14,29].

Our continuous-time mean-field approximation of the exact SIS model for the spreading of a virus in a network, called the N-intertwined model [27], was earlier considered by Ganesh et al. [9] and by Wang et al. [28] in discrete-time, whose paper was later improved in [6]. A remarkable property of the SIS model is the appearance of a phase-transition [4] when the effective infection

* Tel.: +31 152782397.
E-mail address: P.F.A.VanMieghem@tudelft.nl

0140-3664/$ - see front matter © 2012 Elsevier B.V. All rights reserved.
http://dx.doi.org/10.1016/j.comcom.2012.04.015

rate τ approaches the epidemic threshold τ_c^*. Below the epidemic threshold τ_c^*, the network is virus-free in the meta-stable state,[1] while above τ_c^*, there is always a fraction of nodes that remains infected. The determination of the precise epidemic threshold τ_c^* in any network is a long-standing open, difficult problem and a major contribution of the mean-field N-intertwined model is the lower bound $\tau_c = \frac{1}{\lambda_1} \leqslant \tau_c^*$, where λ_1 is the largest eigenvalue of the adjacency matrix A, also called the spectral radius. Here, we will complement the analysis of the N-intertwined SIS model inspired by a new metric, the viral conductance ψ, introduced in [11,29] and reviewed in Section 3. The viral conductance ψ, precisely defined in (17), measures the integrated effect over all possible viral infection strengths on the network's infectious vulnerability. This paper is part of a larger study on network robustness [25], in which a framework is proposed to assess the level of robustness of a given network, based on network metrics. As argued in Section 3, the vulnerability of a network against epidemics should be measured by a set of metrics including the epidemic threshold $\tau_c = \frac{1}{\lambda_1}$ and the viral conductance ψ, rather than only by the epidemic threshold, because ψ complements τ_c naturally. Other possible viral metrics can be taken into account as well, since any proposal of a metric can be motivated or debated. However, as pointed out in [25], a relevant and desirable set of network metrics should be small and consisting of as independent[2] as possible metrics.

Finally, we point here to another dynamic process on a network, that bears resemblance to virus spread. The synchronization of coupled oscillators in a network features a surprisingly similar phase transition: the onset of oscillator coupling occurs [17] at a critical coupling strength $g_c = \frac{g_0}{\lambda_1}$ and the behavior of the phase transition around g_c is mathematically similar [24] to that of the epidemic threshold τ_c. Synchronization [19] plays a role in sensor networks, human body (hart beat, brain, epilepsy), light emission of fire-flies, etc. In Section 3, we propose the analogue of the viral conductance, namely the synchronizability of a network, that measures the ease in which coupled oscillators in a certain network synchronize for all possible coupling strengths. The inspiring analogy between virus spread and synchronization in networks may open new avenues: we speculate that results here obtained for the viral conductance may translate to the setting of coupled oscillators in a network.

The outline of the paper is as follows. First, we review the N-intertwined SIS virus spread model in Section 2 and derive series expansion around the epidemic threshold τ_c and around $\tau \to \infty$ in Section 4 that will be used to express the viral conductance ψ as a series in Section 5. Section 6 gives analytic bounds for ψ, while Section 7 explains theoretically an observation from simulations in [29]: the steady-state fraction y_∞ of infected nodes in the steady-state around $\tau \simeq \frac{N}{L}$ is about $y_\infty \simeq \frac{1}{2}$, where N is the number of nodes and L is the number of links in the network. Proofs are placed in the Appendix. Apart from the overview in Section 2, the presented analytic results in the subsequent sections are new and add to the general theory of the N-intertwined model in [27].

2. The *N*-intertwined SIS model in brief

In contrast to all published SIS-type of models, the N-intertwined model, proposed and investigated in depth in [27] and reviewed in [23], only makes 1 (mean-field) approximation in the exact SIS model and is applicable to all graphs. In [15,5], we show that the mean-field approximation *upper bounds* the exact $\Pr[X_i(t) = 1]$ (which is useful to guarantee epidemic safety bounds in real networks) and that it implies that the random variables X_j and X_i are implicitly assumed to be independent. Since this basic assumption is increasingly good for large N, we expect that the deductions from the N-intertwined model in sufficiently dense networks (i.e. with average degree increasing with N) are asymptotically (for $N \to \infty$) nearly exact. The homogenous N-intertwined model, where the infection and curing rate is the same for each link and node in the network, has been extended to a heterogeneous setting in [26], where each node i has its own infection rate β_i and curing rate δ_i. Furthermore, the method and analysis of the N-intertwined model has been transferred to the SIR model in [30], while in [7], the N-intertwined model is extented to an SAIS infection, where the Alert (A) state is introduced next to the S ($X_i = 0$) and I ($X_i = 1$) state. A very general extension of the N-intertwined model is proposed in [18], while second order mean-field improvements are studied in [5]. The N-intertwined model is shown in [12] to be generally superior to another widely used mean-field model, the heterogeneous mean-field model of Pastor-Satorras and Vespignani [16].

2.1. Governing equations

We briefly summarize the key aspects of the N-intertwined model. The governing differential equation in the N-intertwined model for a node i is

$$\frac{dv_i(t)}{dt} = \beta(1 - v_i(t))\sum_{j=1}^{N} a_{ij} v_j(t) - \delta v_i(t) \tag{1}$$

In words, the time-derivative of the infection probability of a node i consists of two competing processes: (1) while healthy with probability $(1 - v_i(t))$, all infected neighbors, with an average number of $\sum_{j=1}^{N} a_{ij} v_j(t)$, try to infect the node i with rate β and (2) while infected with probability $v_i(t)$, the node i is cured at rate δ. Defining the vector $V(t) = [\, v_1(t) \quad v_2(t) \quad \cdots \quad v_N(t)\,]^T$, the matrix representation based on (1) becomes

$$\frac{dV(t)}{dt} = (\beta A - \delta I)V(t) - \beta\,\mathrm{diag}(v_i(t))AV(t) \tag{2}$$

where $\mathrm{diag}(v_i(t))$ is the diagonal matrix with elements $v_1(t), v_2(t), \ldots, v_N(t)$.

In the sequel, we focus on the steady-state where $v_{i\infty} = \lim_{t\to\infty} v_i(t)$ and $\lim_{t\to\infty} \frac{dv_i(t)}{dt} = 0$. From (1), we obtain

$$v_{i\infty} = \frac{\beta\sum_{j=1}^{N} a_{ij} v_{j\infty}}{\beta\sum_{j=1}^{N} a_{ij} v_{j\infty} + \delta} = 1 - \frac{1}{1 + \tau\sum_{j=1}^{N} a_{ij} v_{j\infty}} \tag{3}$$

Beside the trivial solution $v_{i\infty} = 0$, (3) illustrates that there is another positive solution reflecting the meta-stable state in which we are interested here. For regular graphs, where each node has degree d, symmetry in the steady-state implies that $v_{i\infty} = v_\infty$ for all nodes i and it follows from (3) with the definition of the degree $d_i = \sum_{j=1}^{N} a_{ij}$ that

$$v_{\infty;\,\mathrm{regular}} = y_{\infty;\,\mathrm{regular}}(\tau) = 1 - \frac{1}{\tau d} \tag{4}$$

where $y_\infty = \frac{1}{N}\sum_{i=1}^{N} v_{i\infty}$ is the fraction of the average number of infected nodes in the steady-state.

We now provide a couple of new analytic relations that will be used in Section 7. Summing (1) over all i is equivalent to right mul-

[1] Since the exact SIS Markov process has an absorbing state, namely the overall healthy state, the steady-state equals this overall healthy state in which the virus has disappeared from the network. Unfortunately, already for reasonably small networks ($N \geqslant 100$), the time to reach this absorbing state is huge on average (see [8, p. 99]) so that the exact steady-state is hardly ever reached in real networks, while the meta-stable state reflects the observed viral behavior fairly well.The steady-state in the N-intertwined virus spread model refers to the meta-stable state, which is reached exponentially rapidly and which reflects real epidemics more closely.

[2] Since topological metrics (such as the hopcount, clustering coefficient, degree, betweenness, centrality, etc.) are derived from the adjacency matrix A of the network, most of them are correlated [13].

tiplication of $V(t)$ by the all one vector u^T because $\sum_{i=1}^{N} v_i(t) = u^T V(t)$. Then, we find from (2) that

$$\frac{du^T V(t)}{dt} = u^T(\mathrm{diag}(1 - v_i(t))\beta A - \delta I)V(t)$$
$$= \beta(u - V(t))^T A V(t) - \delta u^T V(t)$$

Hence, we obtain a relation for $y_\infty \in [0,1]$ in terms of the vector V_∞:

$$N y_\infty = u^T V_\infty = \tau(u - V_\infty)^T A V_\infty \quad (5)$$

Since the degree vector D satisfies $u^T A = D^T$ because $A = A^T$, we can write (5) as

$$y_\infty(\tau) = \frac{\tau}{N}\left(D^T V_\infty - V_\infty^T A V_\infty\right) \quad (6)$$

Finally, we write the degree vector D as $D = \Delta u$, where $\Delta = \mathrm{diag}(d_1, d_2, \ldots, d_N)$, so that

$$N y_\infty = \tau\left(u^T \Delta V_\infty + V_\infty^T \Delta V_\infty - V_\infty^T \Delta V_\infty - V_\infty^T A V_\infty\right)$$
$$= \tau\left((u - V_\infty)^T \Delta V_\infty + V_\infty^T(\Delta - A)V_\infty\right)$$

Introducing the Laplacian $Q = \Delta - A$ of the graph G, the steady-state fraction of infected nodes y_∞ is expressed as a quadratic form in terms of the Laplacian [22],

$$y_\infty = \frac{\tau}{N}\left((u - V_\infty)^T \Delta V_\infty + V_\infty^T Q V_\infty\right) \quad (7)$$

After left-multiplication of the steady-state version of (2) by the vector $V_\infty^T \mathrm{diag}(v_{i\infty}^{k-1}) = [\, v_{1\infty}^k \quad v_{2\infty}^k \quad \cdots \quad v_{N\infty}^k \,]$, which we denote by $\left(V_\infty^k\right)^T$, we obtain the scalar equation

$$\left(V_\infty^k\right)^T V_\infty = \sum_{j=1}^{N} v_{j\infty}^{k+1} = \tau\left(\left(V_\infty^k\right)^T A V_\infty - \left(V_\infty^{k+1}\right)^T A V_\infty\right) \quad (8)$$

For $k = 0$ in (8), and introducing the all one vector $u = \lim_{k\to 0} V_\infty^k$, we obtain (5) again. For $k = 1$ in (8), the norm $\|V_\infty\|_2^2 = V_\infty^T V_\infty = \sum_{j=1}^{N} v_{j\infty}^2$ obeys

$$V_\infty^T V_\infty = \tau\left(V_\infty^T A V_\infty - V_\infty^T \mathrm{diag}(v_{i\infty}) A V_\infty\right) \quad (9)$$

When summing (8) over all k from $m \geqslant 0$ to infinity and taking $|v_{j\infty}| < 1$ into account the telescoping nature of the right-hand side leads to

$$\sum_{k=m}^{\infty}\left(V_\infty^k\right)^T V_\infty = \sum_{j=1}^{N}\frac{v_{j\infty}^{m+1}}{1 - v_{j\infty}} = \tau(V_\infty^m)^T A V_\infty \quad (10)$$

When $m = 0$, we have that $V_\infty^m = u$ and we obtain, with the degree vector $u^T A = D^T$,

$$\frac{1}{\tau}\sum_{j=1}^{N}\frac{v_{j\infty}}{1 - v_{j\infty}} = D^T V_\infty = \sum_{j=1}^{N} d_j v_{j\infty} \quad (11)$$

As shown earlier in [27], the characteristic structure (10) of the N-intertwined model follows more elegantly from the governing Eq. (2) in the steady-state

$$V_\infty = \tau\,\mathrm{diag}(1 - v_{i\infty}) A V_\infty \quad (12)$$

for finite τ such that $v_{i\infty} < 1$. Indeed, after left-multiplying both sides by $(\mathrm{diag}(1 - v_{i\infty}))^{-1} = \mathrm{diag}\left(\frac{1}{1 - v_{i\infty}}\right)$, we have

$$\frac{1}{\tau}\mathrm{diag}\left(\frac{1}{1 - v_{i\infty}}\right) V_\infty = A V_\infty$$

or

$$\frac{1}{\tau}\frac{V_\infty}{1 - V_\infty} = A V_\infty \quad (13)$$

where $\left(\frac{V_\infty}{1 - V_\infty}\right)^T = \left[\frac{v_{1\infty}}{1 - v_{1\infty}} \quad \frac{v_{2\infty}}{1 - v_{2\infty}} \quad \cdots \quad \frac{v_{N\infty}}{1 - v_{N\infty}}\right]$. By left-multiplication of (13) by $(V_\infty^m)^T$, we obtain (10) again.

2.2. An eigenvector approach

Since the eigenvectors $x_1, x_2, \ldots, x_N$ belonging to the eigenvalues $\lambda_1 \geqslant \lambda_2 \geqslant \cdots \geqslant \lambda_N$ of the adjacency matrix A span the N-dimensional vector space, we can write the steady-state infection probability vector $V_\infty(\tau)$ as a linear combination of the eigenvectors of A,

$$V_\infty(\tau) = \sum_{k=1}^{N}\gamma_k(\tau) x_k \quad (14)$$

where the coefficient $\gamma_k(\tau) = x_k^T V_\infty(\tau)$ is the scalar product of $V_\infty(\tau)$ and the eigenvector x_k and where the eigenvector x_k obeys the normalization $x_k^T x_k = 1$. Physically, (14) maps the dynamics $V_\infty(\tau)$ of the process onto the eigenstructure of the network, where $\gamma_k(\tau)$ determines the importance of the process in a certain eigendirection of the graph. The definition $y_\infty(\tau) = \frac{1}{N} u^T V_\infty(\tau)$ shows that

$$y_\infty(\tau) = \frac{1}{N}\sum_{k=1}^{N}\gamma_k(\tau) u^T x_k \quad (15)$$

Substitution of (14) into (5) yields

$$y_\infty(\tau) = \frac{\tau}{N}\sum_{k=1}^{N}\lambda_k\gamma_k(\tau)(u^T x_k - \gamma_k(\tau)) \quad (16)$$

For irregular graphs, generally, $\gamma_m(\tau) = x_m^T V_\infty(\tau) \neq 0$ for $m > 1$ and all eigenvalues and eigenvectors in (16) play a role. Moreover, $\gamma_m(\tau)$ can be negative, as well as λ_m, while $\sum_{k=1}^{N}\lambda_k = 0$ (see [22, p. 30]). The larger the spectral gap $\lambda_1 - \lambda_2$ and the smaller $|\lambda_N|$, the more y_∞ is determined by the dominant $k = 1$ term in (16), and the more its viral behavior approaches that of a regular graph. Graphs with large spectral gap possess strong topological robustness [22], in the sense that it is difficult to tear that network apart.

3. The viral conductance

The viral conductance ψ of a virus spreading process in a graph was first proposed in [11] as a new graph metric and then elaborated in more detail in [29]. The viral conductance ψ is defined as

$$\psi = \int_0^{\lambda_1} y_\infty(s)\,ds \quad (17)$$

where $s = \frac{1}{\tau}$. Below the epidemic threshold τ_c, the network is virus-free in the steady-state. Hence, $v_{i\infty}(\tau) = 0$ for $\tau < \tau_c$, and equivalently, $v_{i\infty}(s) = 0$ for $s > \frac{1}{\tau_c} = \lambda_1$. Since the function $y_\infty(\tau)$ versus τ is not integrable over all τ, Kooij et al. [11] have proposed to consider $y_\infty(\frac{1}{\tau})$ versus $s = \frac{1}{\tau}$. Fig. 1 illustrates the typical behavior of $y_\infty(s)$ versus $s = \frac{1}{\tau}$ and $y_\infty(\tau)$ versus τ in the insert for a regular and irregular graph. Theoretically – though debatable – one might argue that the effective curing rate $s = \frac{\delta}{\beta} = \frac{1}{\tau}$ is more natural than the effective infection rate $\tau = \frac{\beta}{\delta}$, because a Taylor expansion of $y_\infty(s)$ around $s = 0$ can be deduced, while the corresponding one for $y_\infty(\tau)$ is a Laurent series in $\frac{1}{\tau}$ around $\tau \to \infty$ (see Lemma 2).

In most published work so far, network G_1 was considered to be more robust against virus spread than network G_2 if the epidemic threshold $\tau_c(G_1) > \tau_c(G_2)$. For example, in Fig. 1, the regular graph with the same number N of nodes and nearly the same number L of links possesses a higher epidemic threshold than the star, and, thus, according to the above robustness criterion, the regular graph is more robust against virus propagation than the star. However,

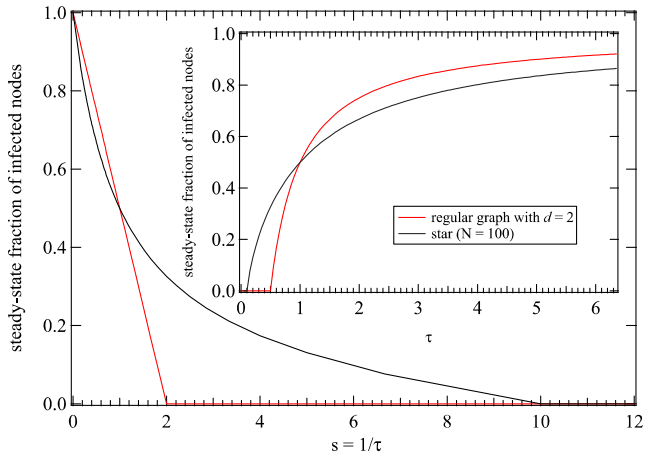

Fig. 1. The steady-state fraction y_∞ of infected nodes versus $s = 1/\tau$ (and versus τ in the insert) for a regular graph with degree $d = 2$ and a star with $N = 100$ nodes. Both graphs have almost the same average degree.

when the effective infection rate $\tau > 1 = 2\tau_c(G_{\text{regular}})$, we observe from Fig. 1 that the percentage of infected nodes in the star is smaller than in the regular graph. The extent of the virus-free region is one aspect of the network's resilience against viruses, but once that barrier, the epidemic threshold, is crossed, the virus may conduct differently in networks with high and low epidemic threshold. This observation has led Kooij et al. [11] to propose the viral conductance as an additional metric. As mentioned in Section 1, robustness metrics should be as complementary as possible. The sensitivity or dependence of the viral conductance ψ on the epidemic threshold τ_c could be assessed by

$$\frac{d\psi}{d\lambda_1} = \int_0^{\lambda_1} \frac{\partial y_\infty(s)}{\partial \lambda_1} ds$$

which is difficult to compute or by correlation simulations. Such simulations on scale-free, Erdős–Rényi and small-world graphs indicate the relatively low correlation.

The viral conductance ψ is a graph metric that represents the overall conductance of the virus for all possible effective infection rates τ: when ψ is high for the graph G, the virus can spread easily in G. Thus, instead of grading graphs only based on their epidemic threshold τ_c from virus vulnerable, where τ_c is small (high spectral radius λ_1) to virus robust (where τ_c is large), the viral conductance complements this classification with an average infection notion because

$$\overline{y_\infty} = \frac{1}{\lambda_1} \int_0^{\lambda_1} y_\infty(s) ds < 1$$

so that $\psi = \frac{\overline{y_\infty}}{\tau_c} < \frac{1}{\tau_c} = \lambda_1$. Graphs with small epidemic threshold may possess a small average fraction of infected nodes $\overline{y_\infty}$ so that the viral conductance can be equal to graphs with large epidemic threshold and large $\overline{y_\infty}$.

The concept of viral conductance can be transferred to the synchronization of coupled oscillators in a network [17]. The dynamic coupling of oscillators (nodes) is comparable to virus spread in networks: there is a critical coupling strength $g_c = \frac{g_0}{\lambda_1}$, where g_0 is a constant and the behavior of the phase transition around g_c is mathematically similar [24]. The direct translation of the viral conductance to the synchronizability S of a network is defined as

$$S = \int_0^{\lambda_1} r^2(u) du$$

where $u = \frac{1}{g}$ and r is the order parameter [17] instead of the fraction of coupled or phase-locked oscillators. Thus, the analogue of the effective infection rate τ is the coupling strength g, the epidemic threshold $\tau_c = \frac{1}{\lambda_1}$ corresponds to the onset of synchronization $g_c = \frac{g_0}{\lambda_1}$, while the steady-state fraction of infected nodes y_∞ translates to the order parameter r^2. Similar to ψ, the synchronizability S measures the ease in which a set of oscillators in a given network synchronize for all possible coupling strengths g: the higher S, the easier oscillator nodes in a network synchronize. The synchronizability S plays a same role as the viral conductance and can be used to distinguish between networks. In particular in medical sciences, a high synchronizability S of the functional brain network would indicate that the patient is vulnerably for epileptic seizures.

3.1. Some exact expressions for ψ

For regular graphs with degree d, the basic relation (4) for $y_{\infty;\text{regular}}$ shows that the viral conductance equals

$$\psi_{\text{regular}} = \int_0^d \left(1 - \frac{s}{d}\right) ds = \frac{d}{2} = \frac{L}{N}$$

which is independent of the size N of the network!

For the complete bipartite graph $K_{m,n}$, where there are two partitions $\mathcal{N}_m$ with m nodes and $\mathcal{N}_n$ with n nodes so that $N = m + n$ and $L = mn$, we have [27] that

$$v_{i\infty} = \frac{mn - \frac{1}{\tau^2}}{(\frac{1}{\tau} + m)n} \quad i \in \mathcal{N}_n \tag{18}$$

and

$$v_{j\infty} = \frac{mn - \frac{1}{\tau^2}}{(\frac{1}{\tau} + n)m} \quad j \in \mathcal{N}_m \tag{19}$$

Since $y_\infty(s) = \frac{n v_{i\infty} + m v_{j\infty}}{n+m}$, we obtain

$$y_\infty(s) = \frac{(mn - s^2)}{N}\left(\frac{1}{s+m} + \frac{1}{s+n}\right) \tag{20}$$

and, with $\lambda_1(K_{m,n}) = \sqrt{mn}$ (see [22, p. 130]), the viral conductance of the complete bipartite graph $K_{n,m}$ equals

$$\psi_{K_{n,m}} = \frac{1}{N} \int_0^{\sqrt{mn}} \left(\frac{mn - s^2}{s+m} + \frac{mn - s^2}{s+n}\right) ds$$

Using $\int \frac{A - s^2}{s+m} ds = (A - m^2)\log(s+m) - \frac{s^2}{2} + ms + c$, where c is a constant, we obtain

$$\psi_{K_{n,m}} = \sqrt{mn} - \frac{mn}{N} + \frac{(n-m)}{N} \log \frac{\left(1 + \sqrt{\frac{n}{m}}\right)^m}{\left(1 + \sqrt{\frac{m}{n}}\right)^n} \tag{21}$$

Notice the symmetry in (21), namely that $\psi_{K_{n,m}} = \psi_{K_{m,n}}$. Also, if $m = n$, we again obtain a regular graph, for which $\psi_{K_{n,n}} = \frac{n}{2}$. The other extreme occurs for a star $K_{1,n}$, where $m = 1$ and $n = N - 1$ in (21). After some tedious manipulations, we obtain

$$\psi_{\text{star}} = \frac{\log N}{2} - \frac{1}{2} + O\left(\frac{1}{\sqrt{N}}\right) \tag{22}$$

The cycle, which is a regular graph with degree $d = 2$, only has $\psi_{\text{cycle}} = 1$, irrespective of the number N of nodes. Given a fixed number N of nodes, the viral conductance $\psi_{K_{n,N-n}}$ (as well as the number $L = n(N-n)$ of links) increases with n from $n = 1$ (star) up to $n = \frac{N}{2}$ (a regular graph). When both N and the average degree $E[D] = \frac{2L}{N}$ are fixed, the following lemma is proved in Appendix E:

Lemma 1. *For a given N and L, the viral conductance of the complete bipartite graph $K_{m,n}$ is minimal when it is regular ($m = n$).*

4. Derivatives of $y_\infty(s)$ at $s = 0$ and $s \to \lambda_1$

Extremely high effective infection rates ($\tau \to \infty$) correspond to $s = 0$ at which $y_\infty(s) = 1$ and below the epidemic threshold, $\tau < \tau_c$ or $s > s_c = \lambda_1$, $y_\infty(s) = 0$. Besides these two points, the derivative at $\lim_{s\to 0} \frac{dy_\infty(s)}{ds}$ and $\lim_{s\to\lambda_1} \frac{dy_\infty(s)}{ds}$ can be computed exactly, as shown here for the first time. This section provides new series expansion for the viral steady-state probabilities $v_{i\infty}$, which will be used in Section 5 to bound the viral conductance ψ.

The following Lemma 2 is proved in Appendix C.

Lemma 2. *The Laurent series of the steady-state infection probability*

$$v_{i\infty}(\tau) = 1 + \sum_{m=1}^{\infty} \eta_m(i)\tau^{-m} \tag{23}$$

possesses the coefficients

$$\eta_1(i) = -\frac{1}{d_i} \tag{24}$$

and

$$\eta_2(i) = \frac{1}{d_i^2}\left(1 - \sum_{j=1}^{N} \frac{a_{ij}}{d_j}\right) \tag{25}$$

and for $m \geqslant 2$, the coefficients obey the recursion

$$\eta_{m+1}(i) = -\frac{1}{d_i}\eta_m(i)\left(1 - \sum_{j=1}^{N} \frac{a_{ij}}{d_j}\right) - \frac{1}{d_i}\sum_{k=2}^{m} \eta_{m+1-k}(i) \sum_{j=1}^{N} a_{ij}\eta_k(j) \tag{26}$$

For regular graphs with degree d, we observe that $\eta_1(i) = \eta_1 = -\frac{1}{d}$ and $\eta_m(i) = 0$ for all $m > 1$, which is in agreement with (4). From the Laurent series (23) in Lemma 2 after the transform $s = \frac{1}{\tau}$, the derivative at $\lim_{s\to 0} \frac{dy_\infty(s)}{ds}$ can be computed exactly as

$$\lim_{s\to 0} \frac{dy_\infty(s)}{ds} = -\frac{1}{N}\sum_{j=1}^{N} \frac{1}{d_j} = -E\left[\frac{1}{D}\right] \tag{27}$$

which is minus the harmonic mean of the degrees in the graph. The harmonic, geometric and arithmetic mean inequality (see e.g. [22, p. 138]) shows[3] that

$$E\left[\frac{1}{D}\right] = \frac{1}{N}\sum_{j=1}^{N} \frac{1}{d_j} \geqslant \frac{1}{E[D]} \geqslant \frac{1}{\lambda_1}$$

with equality for the regular graph. Hence, the slope $\lim_{s\to 0} \frac{dy_\infty(s)}{ds}$ is the least steep for the regular graph as also illustrated in Fig. 1. We also mention that (27) has been inferred in [27] based on simulations, but not rigorously proved as here.

While the right-derivative[4] $\lim_{s\downarrow\lambda_1} \frac{dy_\infty(s)}{ds} = 0$, the left-derivative at $\lim_{s\uparrow\lambda_1} \frac{dy_\infty(s)}{ds}$ can be computed explicitly from the following theorem, proved in [24]:

Theorem 3. *For any graph with spectral radius λ_1 and corresponding eigenvector x_1 normalized such that $x_1^T x_1 = \sum_{j=1}^{N} (x_1)_j^2 = 1$, the steady-state fraction of infected nodes y_∞ obeys*

$$y_\infty(\tau) = \frac{1}{\lambda_1 N}\frac{\sum_{j=1}^{N}(x_1)_j}{\sum_{j=1}^{N}(x_1)_j^3}\left(\tau_c^{-1} - \tau^{-1}\right) + O\left(\tau_c^{-1} - \tau^{-1}\right)^2 \tag{28}$$

when τ approaches the epidemic threshold τ_c from above.

From (28), we have

$$\left.\frac{dy_\infty(s)}{ds}\right|_{s=\lambda_1} = -\frac{1}{\lambda_1 N}\frac{\sum_{j=1}^{N}(x_1)_j}{\sum_{j=1}^{N}(x_1)_j^3} \tag{29}$$

which is shown in [24] to be bounded as

$$-\frac{1}{\lambda_1} \leqslant \left.\frac{dy_\infty}{ds}\right|_{s\uparrow\lambda_1} \leqslant \frac{1}{\lambda_1 N \max_{1\leqslant j\leqslant N}(x_1)_j} < 0 \tag{30}$$

Theorem 3 suggests, for all $1 \leqslant k \leqslant N$, the existence of the power series

$$\gamma_k(\tau) = \sum_{j=1}^{\infty} c_j(k)\left(\tau_c^{-1} - \tau^{-1}\right)^j \tag{31}$$

where $c_1(k) = 0$ for $2 \leqslant k \leqslant N$ and $c_1(1) = \left(\lambda_1 \sum_{j=1}^{N}(x_1)_j^3\right)^{-1}$. In particular, from the definition (15), we obtain the series expansion of $y_\infty(\tau)$ around $\tau_c^{-1} - \tau^{-1}$ as

$$y_\infty(\tau) = \frac{1}{N}\sum_{j=1}^{\infty}\sum_{k=1}^{N} c_j(k) u^T x_k \left(\tau_c^{-1} - \tau^{-1}\right)^j \tag{32}$$

valid for $\tau \geqslant \frac{1}{\lambda_1}$. Similarly, from the eigenvector expansion (14), all steady-state infection probabilities $v_{i\infty}(\tau)$ are expanded as

$$v_{i\infty}(\tau) = \sum_{j=1}^{\infty}\sum_{k=1}^{N} c_j(k)(x_k)_i\left(\tau_c^{-1} - \tau^{-1}\right)^j \tag{33}$$

We extend the above analysis and determine all coefficients $c_j(k)$ in a recursive way as specified in Lemma 4, which is proved in Appendix D.

Lemma 4. *Defining*

$$X(m,l,k) = \sum_{q=1}^{N} (x_m)_q (x_l)_q (x_k)_q$$

the coefficients $c_j(m)$ in (31) obey, for $m > 1$ and $j > 2$, the recursion

$$\begin{aligned} c_j(m) = {} & \frac{c_{j-1}(m)}{\lambda_1 - \lambda_m}\{1 - c_1(1)(\lambda_1 + \lambda_m)X(m,m,1)\} \\ & - \frac{c_1(1)}{\lambda_1 - \lambda_m}\sum_{k=1;k\neq m}^{N} (\lambda_1 + \lambda_k)c_{j-1}(k)X(m,k,1) \\ & - \frac{1}{\lambda_1 - \lambda_m}\sum_{n=2}^{j-2}\sum_{l=1}^{N}\sum_{k=1}^{N} c_{j-n}(l)c_n(k)\lambda_k X(m,l,k) \end{aligned} \tag{34}$$

while, for $j = 2$ and $m > 1$,

$$c_2(m) = -\frac{1}{\lambda_1 - \lambda_m}\frac{X(m,1,1)}{\lambda_1 X^2(1,1,1)} \tag{35}$$

and $c_1(m) = 0$. For $m = 1$, there holds that $c_1(1) = \left(\lambda_1 \sum_{j=1}^{N}(x_1)_j^3\right)^{-1}$ and for $j > 1$, the coefficients $c_j(1)$ satisfy the recursion

$$\begin{aligned} c_j(1) = {} & -\frac{1}{\lambda_1 X(1,1,1)}\sum_{k=2}^{N}(\lambda_1 + \lambda_k)c_j(k)X(1,1,k) \\ & - \sum_{n=2}^{j-1}\sum_{l=1}^{N}\sum_{k=1}^{N} c_{j+1-n}(l)c_n(k)\lambda_k X(1,l,k) \end{aligned} \tag{36}$$

The radius of convergence of the Laurent series (23) and of the series (31) is, in general, unknown and still an open problem. In addition to Theorem 3, we present an orthogonality condition, proved in Appendix B, for the derivative of the vector V_∞ defined as $\frac{dV_\infty^T}{ds} = \left[\frac{dv_{1\infty}}{ds} \quad \frac{dv_{2\infty}}{ds} \quad \cdots \quad \frac{dv_{N\infty}}{ds}\right]^T$ at $s = \lambda_1$:

Lemma 5. *In any graph, the vector $\left.\frac{dV_\infty}{ds}\right|_{s=\lambda_1}$ is orthogonal to the vector $D - \lambda_1 u$.*

[3] Since $f(x) = \frac{1}{x}$ is convex for $x > 0$, Jensen's inequality [21], $f(E[X]) \leqslant E[f(X)]$, applies as well.

[4] The notation $\lim_{x\downarrow x_0} f(x)$ is the limit towards x_0 when x approaches x_0 from above, i.e. $x > x_0$.

Expression (28) illustrates that, among all graphs with N nodes and L links, the regular graph with degree $d = \frac{2L}{N}$ has the largest epidemic threshold $\tau_c = \frac{1}{d}$, but also the largest (in absolute value) derivative $\left.\frac{dy'_\infty}{ds}\right|_{s\to\lambda_1} = -\frac{1}{\lambda_1} = -\frac{1}{d}$ because equality in (30) is reached. This means that a higher effective infection rate τ is needed to cause a non-zero steady-state fraction of nodes in the regular graph to be permanently infected, but that, slightly above that critical rate τ_c, a higher relative fraction of nodes is infected than in other graphs. In other words, the change in virus conductivity at $\tau = \tau_c + \epsilon$ is highest in regular graphs. Thus, when we are asked to classify networks according to their proneness to viral infections, the epidemic threshold alone is insufficient as metric alone. Our analysis based on Theorem 3 supports the viral conductance ψ as an additional candidate metric that complements the epidemic threshold $\tau_c = \frac{1}{\lambda_1}$.

5. Analysis of the viral conductance ψ

As in [29], one may device heuristics to approximate the steady-state fraction of infected nodes $y_\infty(s)$ in the s-interval $[0, \lambda_1]$ based on the two endpoints, their derivative and on the convexity[5] of $y_\infty(s)$. Strict convexity (for irregular graphs) also means that the derivative $\frac{dy_\infty}{ds}$ decreases from $s = 0$ up to $s = \lambda_1$ consistent with both Lemma 2 and Theorem 3. Here, we present an analysis of the viral conductance ψ using the knowledge of $y_\infty(\lambda_1) = 0, y_\infty(0) = 1$ and the corresponding derivatives, $y'_\infty(\lambda_1)$ and $y'_\infty(0)$ specified in Section 4, together with the convexity of $y_\infty(s)$.

Since $y_\infty(s) \leqslant 1$, we obtain the trivial upper bound $\psi \leqslant \lambda_1$ for the viral conductance (17). Convexity of $y_\infty(s)$ implies that $y_\infty(s) \leqslant 1 - \frac{s}{\lambda_1}$ from which the sharper upper bound

$$\psi \leqslant \frac{\lambda_1}{2}$$

is immediate.

After partial integration, the definition of the viral conductance (17) becomes, for any real x,

$$\psi = \int_0^{\lambda_1} y_\infty(s)ds = x - \int_0^{\lambda_1} (s-x)y'_\infty(s)ds$$

Again partially integrating yields

$$\psi = x + \frac{1}{2}x^2 y'_\infty(0) - \frac{1}{2}(\lambda_1 - x)^2 y'_\infty(\lambda_1) + \frac{1}{2} \times \int_0^{\lambda_1} (s-x)^2 y''_\infty(s)ds \quad (37)$$

Convexity, i.e. $y''_\infty(s) \geqslant 0$ with equality only for regular graphs, implies that

$$\psi \geqslant f(x) = x + \frac{1}{2}x^2 y'_\infty(0) - \frac{1}{2}(\lambda_1 - x)^2 y'_\infty(\lambda_1) = \{1 + y'_\infty(\lambda_1)\lambda_1\}x + \frac{1}{2}x^2\{y'_\infty(0) - y'_\infty(\lambda_1)\} - \frac{1}{2}y'_\infty(\lambda_1)\lambda_1^2$$

Furthermore,

$$f'(x) = 1 + xy'_\infty(0) + (\lambda_1 - x)y'_\infty(\lambda_1)$$

while

$$f''(x) = y'_\infty(0) - y'_\infty(\lambda_1) < 0$$

demonstrates that the solution of $f'(\zeta) = 0$, i.e.

$$\zeta = -\frac{1 + \lambda_1 y'_\infty(\lambda_1)}{y'_\infty(0) - y'_\infty(\lambda_1)}$$

generates a maximum

$$f(\zeta) = -\frac{1}{2}y'_\infty(\lambda_1)\lambda_1^2 - \frac{1}{2}\frac{\left(1 + \lambda_1 y'_\infty(\lambda_1)\right)^2}{y'_\infty(0) - y'_\infty(\lambda_1)}$$

Thus, for irregular graphs, our optimized lower bound for ψ is

$$\psi \geqslant \frac{\lambda_1^2}{2}\left(-y'_\infty(\lambda_1)\right) + \frac{1}{2}\frac{\left(1 - \lambda_1\left(-y'_\infty(\lambda_1)\right)\right)^2}{|y'_\infty(0) - y'_\infty(\lambda_1)|}$$

Explicitly, with (27) and (29),

$$\psi \geqslant \frac{\lambda_1}{2}\left(Z + \frac{(1-Z)^2}{|\lambda_1 E[\frac{1}{D}] - Z|}\right) \quad (38)$$

where $Z = \frac{1}{N}\frac{\sum_{j=1}^N (x_1)_j}{\sum_{j=1}^N (x_1)_j^3}$ and $\zeta = \frac{1-Z}{\lambda_1 E[\frac{1}{D}] - Z} \leqslant 1$ because $\lambda_1 E[\frac{1}{D}] \geqslant \frac{\lambda_1}{E[D]} \geqslant 1$. Equality in (38) occurs for regular graphs where $Z = 1$ and $\lambda_1 = d$. With the bounds for irregular graphs

$$\frac{1}{N\max 1 \leqslant j \leqslant N(x_1)_j} < Z < 1$$

we see that the second term in (38) is, indeed, a small correction.

The general form (37) shows that the lower bound (38) can be sharpened by adding

$$\int_0^{\lambda_1} \frac{(s-x)^2}{2} y''_\infty(s)ds > \frac{1}{2}\min_{s\in[0,\lambda_1]} y''_\infty(s)\int_0^{\lambda_1}(s-x)^2 ds = \frac{\lambda_1}{2}\min_{s\in[0,\lambda_1]} y''_\infty(s)\left(\frac{\lambda_1^2}{3} - \lambda_1 x + x^2\right)$$

evaluated at $x = \zeta < 1$ because $\frac{\lambda_1^2}{3} - \lambda_1\zeta + \zeta^2 > 0$ when $\lambda_1 \geqslant 3$. In summary, we arrive at

$$\psi \geqslant \frac{\lambda_1}{2}\left\{Z + \zeta(1-Z) + \min_{s\in[0,\lambda_1]} y''_\infty(s)\left(\frac{\lambda_1^2}{3} - \lambda_1\zeta + \zeta^2\right)\right\} \quad (39)$$

Similarly, a same type of upper bound follows directly as

$$\psi \leqslant \frac{\lambda_1}{2}\left\{Z + \zeta(1-Z) + \max_{s\in[0,\lambda_1]} y''_\infty(s)\left(\frac{\lambda_1^2}{3} - \lambda_1\zeta + \zeta^2\right)\right\} \quad (40)$$

For the complete bipartite graph $K_{n,m}$, the second derivative of (20) equals

$$y''_\infty(s) = \frac{2(m-n)^2\left(m^2 n - s^3 + mn(n+3s)\right)}{(m+n)(m+s)^3(n+s)^3}$$

and $\min_{s\in[0,\lambda_1]} y''_\infty(s) = y''_\infty(\lambda_1) = \frac{2(m-n)^2}{(m+n)\sqrt{mn}\left(\sqrt{m}+\sqrt{n}\right)^4}$ and $\max_{s\in[0,\lambda_1]} y''_\infty(s) = y''_\infty(0) = \frac{2(m-n)^2}{m^2 n^2}$. The ratio $\frac{y''_\infty(0)}{y''_\infty(\lambda_1)} = \left(1+\frac{n}{m}\right)\sqrt{\frac{n}{m}}\left(1+\sqrt{\frac{m}{n}}\right)^4$ increases with increasing irregularity, i.e. with increasing ratio $\frac{n}{m}$. The class of complete bipartite graphs can range from regularity $m = n$ to extreme irregularity in the star, where $m = 1$ and $n = N - 1$. Therefore, that class of $K_{n,m}$ is our benchmark.

If the right-hand side in (39) can be shown to exceed $\frac{1}{2}E[D] = \frac{L}{N}$, then it would imply that the viral conductance of the regular graph is the smallest among all graphs with N nodes and L links. Lemma 1 states that the claim holds for the class of complete bipartite graphs and simulations in [29] suggest the truth of the claim for other types of graphs as well.

[5] A long the same lines as in [26], we can prove that $v_{j\infty}(s)$ is (strict) convex in s, for $s < s_c$.

5.1. Series expansions for the viral conductance ψ

When using the Laurent expansion in (23), the steady-state fraction of infected nodes can be formally written as

$$y_\infty(s) = 1 + \frac{1}{N}\sum_{m=1}^{\infty}\sum_{i=1}^{N}\eta_m(i)s^m$$

while (32) yields

$$y_\infty(s) = \frac{1}{N}\sum_{j=1}^{\infty}\sum_{k=1}^{N}c_j(k)u^T x_k(\lambda_1 - s)^j$$

We write the integral in (17) as

$$\psi = \int_0^{\frac{\lambda_1}{2}} y_\infty(s)ds + \int_{\frac{\lambda_1}{2}}^{\lambda_1} y_\infty(s)ds$$

and use the expansion around $s = 0$ in the first and the other expansion in the second integral to obtain

$$\psi = \frac{\lambda_1}{2} + \frac{1}{N}\sum_{m=1}^{\infty}\sum_{k=1}^{N}(\eta_m(k) + c_m(k)u^T x_k)\frac{\lambda_1^{m+1}}{2^{m+1}(m+1)}$$

This series for ψ is valid provided the convergence radius of both series for $y_\infty(s)$ is at least $\frac{\lambda_1}{2}$. Executing the first term yields

$$\begin{aligned}\psi &= \frac{\lambda_1}{2} - \frac{1}{N}\left(\sum_{k=1}^{N}\frac{1}{d_k} - \frac{u^T x_1}{\lambda_1\sum_{j=1}^{N}(x_1)_j^3}\right)\frac{\lambda_1^2}{8} + R_2\\ &= \frac{\lambda_1}{2}\left\{1 - \frac{1}{4}\left(\lambda_1 E\left[\frac{1}{D}\right] - Z\right)\right\} + R_2\end{aligned}$$

where the remainder R_2 is

$$R_2 = \frac{1}{N}\sum_{m=2}^{\infty}\sum_{k=1}^{N}(\eta_m(k) + c_m(k)u^T x_k)\frac{(\lambda_1)^{m+1}}{2^{m+1}(m+1)}$$

Subject to the above convergence condition, both expansions can be numerically computed up to any desired accuracy when the adjacency matrix A is given, from which the spectral expression $A = X\Lambda X^T$ can be computed [22].

6. Bounds for the viral conductance

In addition to the upper (40) and lower bound (39) derived in Section 5 and based on derivatives of $y_\infty(s)$, we here present other types of upper and lower bounds that lead to relatively simple expressions in terms of graph properties.

6.1. Upper bounds for the viral conductance

By exploiting Theorem 9, proved in [27] and alternatively in Appendix A, considerably sharper bounds can be deduced. Each convergent of the continued fraction expansion (50) provides an upper bound for $v_{i\infty}$. The first convergent of (50),

$$v_{i\infty} \leqslant 1 - \frac{1}{1+\tau d_i}$$

leads to

$$y_\infty(s) \leqslant 1 - \frac{1}{N}\sum_{i=1}^{N}\frac{1}{1+\frac{d_i}{s}}$$

Hence, the viral conductance is bounded by

$$\begin{aligned}\psi &\leqslant \int_0^{\lambda_1}\left(1 - \frac{1}{N}\sum_{i=1}^{N}\frac{1}{1+\frac{d_i}{s}}\right)ds\\ &= \frac{1}{N}\sum_{i=1}^{N}d_i\ln\left(1+\frac{\lambda_1}{d_i}\right)\end{aligned} \tag{41}$$

For regular graphs, this upper bound (41) translates to $VC_{\text{regular}} \leqslant d\ln 2 = 0.693d$. Also, we deduce from (41) that

$$\psi < \ln\left(1+\frac{\lambda_1}{d_{\min}}\right)\frac{1}{N}\sum_{i=1}^{N}d_i = E[D]\ln\left(1+\frac{\lambda_1}{d_{\min}}\right)$$

where $E[D]$ denotes the average degree.

The second convergent of the continued fraction expansion (50) is

$$v_{i\infty} \leqslant 1 - \frac{1}{1+\tau d_i - \tau\sum_{j=1}^{N}\frac{a_{ij}}{1+\tau d_j}}$$

and the viral conductance is bounded by

$$\begin{aligned}\psi &\leqslant \int_0^{\lambda_1}\left(1 - \frac{1}{N}\sum_{i=1}^{N}\frac{1}{1+\frac{d_i}{s} - \frac{1}{s}\sum_{j=1}^{N}\frac{a_{ij}}{1+\frac{d_j}{s}}}\right)ds\\ &= \lambda_1 - \frac{1}{N}\sum_{i=1}^{N}\int_0^{\lambda_1}\frac{sds}{s+d_i - \sum_{j=1}^{N}\frac{a_{ij}}{s+d_j}}\end{aligned}$$

But this integral cannot be evaluated formally. Instead, we approximate the integral by

$$\int_0^{\lambda_1}\frac{sds}{s+d_i - \sum_{j=1}^{N}\frac{a_{ij}}{s+d_j}} \leqslant \int_0^{\lambda_1}\frac{sds}{s+d_i - \sum_{j=1}^{N}\frac{a_{ij}}{d_j}}$$

and obtain

$$\psi \leqslant \frac{1}{N}\sum_{i=1}^{N}\left(d_i - \sum_{j=1}^{N}\frac{a_{ij}}{d_j}\right)\ln\left(1+\frac{\lambda_1}{d_i - \sum_{j=1}^{N}\frac{a_{ij}}{d_j}}\right) \tag{42}$$

When $d_i - \sum_{j=1}^{N}\frac{a_{ij}}{d_j} = 0$, this i-th term does not contribute to the viral conductance (because $\lim_{x\to 0} x\ln(1+c/x) = 0$).

For a regular graph, this bound simplifies to

$$\begin{aligned}\psi &\leqslant (d-1)\ln\left(1+\frac{d}{d-1}\right)\\ &= (d-1)\left\{\ln 2 + \ln\left(1+\frac{1}{2(d-1)}\right)\right\}\\ &= (d-1)\ln 2 + \sum_{k=1}^{\infty}\frac{(-1)^{k-1}}{k2^k}\frac{1}{(d-1)^{k-1}}\\ &= d\ln 2 - \left(\ln 2 - \frac{1}{2}\right) - \frac{1}{8}\frac{1}{d-1} + O\left(\frac{1}{(d-1)^2}\right)\end{aligned}$$

which is better than the previous bound $\psi \leqslant d\ln 2$. Using

$$\begin{aligned}d_i - \sum_{j=1}^{N}\frac{a_{ij}}{d_j} &\geqslant \min_{1\leqslant i\leqslant N}\left(d_i - \sum_{j=1}^{N}\frac{a_{ij}}{d_j}\right)\\ &\geqslant \min_{1\leqslant i\leqslant N}\left(d_i - \frac{d_i}{d_{\min}}\right) = d_{\min} - 1\end{aligned}$$

in (42), we deduce, for $d_{\min} > 1$, that

$$\psi \leqslant \ln\left(1+\frac{\lambda_1}{d_{\min}-1}\right)\left\{\frac{1}{N}\sum_{i=1}^{N} d_i - \frac{1}{N}\sum_{i=1}^{N}\sum_{j=1}^{N}\frac{a_{ij}}{d_j}\right\}$$
$$< \ln\left(1+\frac{\lambda_1}{d_{\min}-1}\right)\left\{E[D] - \frac{1}{N}\sum_{j=1}^{N}\frac{1}{d_j}\sum_{i=1}^{N} a_{ij}\right\}$$
$$= \ln\left(1+\frac{\lambda_1}{d_{\min}-1}\right)\{E[D]-1\}$$

The viral conductance of the star, where $\lambda_1\left(A_{K_{1,N-1}}\right) = \sqrt{N-1}$ and $E[D] = 2 - \frac{2}{N}$, shows that the logarithmic prefactor can be significant and that ψ can be larger than $E[D]$. In particular, the bound (42) for the star $K_{1,N-1}$ is

$$\psi \lessapprox \frac{\log N}{2} - 2\ln 2 + O\left(\frac{1}{\sqrt{N}}\right)$$

which is correct to first order for large N as verified from (22).

6.2. Lower bound for the viral conductance

Using the lower bound derived in [27], valid for $\tau \geqslant \frac{1}{d_{\min}}$ or $s \leqslant d_{\min}$,

$$1 - \frac{1}{1-\frac{d_i}{d_{\min}} + \tau d_i} \leqslant v_{i\infty}$$

the viral conductance is lower bounded as

$$\psi = \int_0^{d_{\min}} y_\infty(s)ds + \int_{d_{\min}}^{\lambda_1} y_\infty(s)ds$$
$$\geqslant \frac{1}{N}\sum_{j=1}^{N}\int_0^{d_{\min}} v_{i\infty}(s)ds$$

With

$$\int_0^{d_{\min}} v_{i\infty}(s)ds \geqslant \int_0^{d_{\min}}\left(1 - \frac{1}{1-\frac{d_i}{d_{\min}}+\frac{d_i}{s}}\right)ds$$
$$= \frac{d_i d_{\min}}{d_i - d_{\min}}\left\{1 + \frac{d_{\min}}{d_i - d_{\min}}\ln\left(\frac{d_{\min}}{d_i}\right)\right\}$$

we arrive at the lower bound

$$\psi \geqslant \frac{d_{\min}}{N}\sum_{i=1}^{N}\frac{1}{1-\frac{d_{\min}}{d_i}}\left\{1 - \frac{\ln\left(\frac{d_i}{d_{\min}}\right)}{\frac{d_i}{d_{\min}}-1}\right\} \tag{43}$$

Only for regular graphs where $d_i = d_{\min} = d$, equality in the lower bound (43) is achieved, because[6]

$$\int_0^{d_{\min}} v_{i\infty}(s)ds \geqslant \int_0^{d}\left(1-\frac{s}{d}\right)ds = \frac{d}{2}$$

illustrating that the lower bound (43) is the best possible among all graphs. Since the function $1/(1-1/x)\left(1-\frac{\ln x}{x-1}\right)$ is strict increasing from 1/2 for $x = 1$ to 1 when $x \to \infty$, we conclude from (43) that the viral conductance is always larger than the minimum degree $\frac{d_{\min}}{2}$ for non-regular graphs.

In summary, the upper bound (42) and the lower bound (43) provide us with the elegant bounds

$$\frac{d_{\min}}{2} \leqslant \psi < \ln\left(1+\frac{\lambda_1}{d_{\min}-1}\right)\{E[D]-1\}$$

The largest possible ratio $\frac{\lambda_1}{d_{\min}} = O\left(\sqrt{N}\right)$ occurs in the star, which illustrates that the viral conductance is bounded by $\frac{1}{2}E[D]\log N$. Likely, the star possesses the largest viral conductance among all graphs with N nodes and L links.

[6] By taking the limit $d_i \to d_{\min}$ in (43), we find the same result (after invoking de l'Hospital's rule twice).

7. Behaviour of $y_\infty(s)$ around $s = \frac{E[D]}{2}$

Via extensive simulations, Youssef et al. [29] have observed that $y_\infty \simeq \frac{1}{2}$ around $s = \frac{E[D]}{2}$. In this section, we aim to explain these observations. In [15], we have shown, for any graph, that $y_\infty \leqslant \frac{1}{2}$ for $\tau \leqslant \frac{1}{E[D]}$. Here, sharper general bounds are derived.

Lemma 6. *For any graph, it holds that*

$$y_\infty(s) \leqslant \frac{1}{2} + \frac{1}{2}\left(1 - \frac{E[D]}{\lambda_1}\right) \quad \text{for } s = \frac{E[D]}{2} \tag{44}$$

and equality is only possible for the regular graph.

Proof. Convexity of $y_\infty(s)$ for $s \in [0,\lambda_1]$ implies that $y_\infty(qa+(1-q)b) \leqslant qy_\infty(a) + (1-q)y_\infty(b)$ for any $a, b \in [0,\lambda_1]$. By choosing $a = 0$, $b = \lambda_1$ and $(1-q)b = \frac{E[D]}{2}$, we find (44). Equality only holds for the regular graph since only then $y''_\infty(s) = 0$ as verified from (4). □

Lemma 7. *For any graph, it holds that*

$$y_\infty(\tau) \leqslant \tau\left(\frac{E[D]}{4} + \frac{V_\infty^T Q V_\infty}{N}\right) \tag{45}$$

and equality is only possible for the regular graph for which $V_\infty^T Q V_\infty = 0$.

Proof. Consider the Laplacian expression (7) for steady-state fraction of infected nodes y_∞. The Rayleigh principle [22] states that $\mu_N = 0 \leqslant V_\infty^T Q V_\infty \leqslant \mu_1 V_\infty^T V_\infty$, where μ_1 and μ_N are the largest and respectively smallest eigenvalue of the Laplacian Q. The eigenvector u belongs to the smallest eigenvalue $\mu_N = 0$ of Q. Thus, only for regular graphs where each node has degree $d_i = d$ and $V_\infty = v_\infty u$, we observe that $V_\infty^T Q V_\infty = 0$. The first quadratic form in (7)

$$(u - V_\infty)^T \Delta V_\infty = \sum_{j=1}^{N}(1 - v_{j\infty})d_j v_{j\infty}$$

is maximal when, at each node k, $v_{k\infty} = \frac{1}{2}$, resulting in $(u-V_\infty)^T\Delta V_\infty \leqslant \frac{1}{4}\sum_{j=1}^{N} d_j = \frac{L}{2}$. Due to symmetry, this maximum is only reached in the regular graph and (45) is proved. □

Lemma 7 shows for the regular graph that the "tangent" line through the origin ($\tau = 0$) lies above $y_{\infty;\text{regular}}$ and only touches $y_{\infty;\text{regular}}$ at the point $\tau = \frac{2}{E[D]} = \frac{2}{d}$. For any other graph, the slope is not larger than $\frac{E[D]}{4} + \frac{V_\infty^T Q V_\infty}{N}$ and, after transforming $s = \frac{1}{\tau}$ in (45), we find

$$y_\infty(s) \leqslant \frac{1}{2} + \frac{2V_\infty^T Q V_\infty}{NE[D]} \quad \text{for } s = \frac{E[D]}{2} \tag{46}$$

that complements (44). The correction $\frac{1}{2}\left(1 - \frac{E[D]}{\lambda_1}\right)$ in (44) and the correction $\frac{2V_\infty^T Q V_\infty}{NE[D]}$ in (46) are positive and small, but nevertheless show that $y_\infty(s)$ can be larger than $\frac{1}{2}$ at $s = \frac{E[D]}{2}$, as numerically found in [29].

Lemma 8. *For any graph, it holds that*

$$\frac{y_\infty(\tau)}{\tau} \geqslant r(\tau) = \frac{1}{N}\sum_{j=1}^{N} v_{j\infty}\left(d_j - \lambda_1 v_{j\infty}\right) \tag{47}$$

where the lower bound obeys, for any τ,

$$r(\tau) \leqslant \frac{N_2}{4N\lambda_1}$$

and where $N_k = u^T A^k u$ denotes [22] the number of walks of length k.

Proof. The Rayleigh principle [22] and the fact that all involved elements of A and V_∞ are non-negative imply that $0 \leqslant V_\infty^T A V_\infty \leqslant \lambda_1 V_\infty^T V_\infty$, with equality in the upper bound only for the regular graph, where the eigenvalue $\frac{2L}{N} = \lambda_1$ corresponds to the eigenvector u and $V_\infty = v_\infty u$. Hence, (6) is bounded by

$$y_\infty(\tau) \geqslant \frac{\tau}{N}\left(D^T V_\infty - \lambda_1 V_\infty^T V_\infty\right) \tag{48}$$

with equality for the regular graph, from which (47) is immediate. The lower bound $r(\tau)$ in (47) has an extremum at $\tau = \xi > \tau_c$ that obeys

$$\frac{1}{N}\sum_{j=1}^{N} v'_{j\infty}(\xi)\left(d_j - 2\lambda_1 v_{j\infty}(\xi)\right) = 0$$

There are three possible cases: (a) neither all $v'_{j\infty}(\xi) = 0$ nor all $v_{j\infty}(\xi) = \frac{d_j}{2\lambda_1}$, which leads to a complicated, not analytically manageable relation defining ξ; (b) $v'_{j\infty}(\xi) = 0$ for all $1 \leqslant j \leqslant N$, in which case $v_{j\infty}(\xi) = 1$, $\xi \to \infty$ and $\frac{y_\infty(\xi)}{\xi} \to 0$. This case corresponds to a minimum and the lower bound is then negative and, hence, useless; (c) $v_{j\infty}(\xi) = \frac{d_j}{2\lambda_1}$ for each $1 \leqslant j \leqslant N$ in which case the maximum lower bound is attained

$$r(\tau) \leqslant r(\xi) = \frac{1}{4N\lambda_1}\sum_{j=1}^{N} d_j^2 = \frac{N_2}{4N\lambda_1} \tag{49}$$

This demonstrates the lemma. □

We will now estimate the value ξ for which $r(\xi) = \frac{N_2}{4N\lambda_1}$ in irregular graphs where $\mathrm{Var}[D] > 0$. The proof of Lemma 8 shows that $r(\xi)$ attains the maximum bound (49), provided that there exists a value of $\tau = \xi$ for which $v_{j\infty}(\xi) = \frac{d_j}{2\lambda_1}$ for each $1 \leqslant j \leqslant N$, in which case

$$y_\infty(\xi) = \frac{1}{N}\sum_{j=1}^{N}\frac{d_j}{2\lambda_1} = \frac{1}{2\lambda_1}\frac{2L}{N} = \frac{1}{2}\frac{E[D]}{\lambda_1} < \frac{1}{2}$$

Lemma 8 then states that $y_\infty(\xi) \geqslant \frac{\xi N_2}{4N\lambda_1}$ or

$$\frac{1}{\lambda_1}\frac{L}{N} \geqslant \frac{\xi N_2}{4N\lambda_1}$$

from which

$$\xi \leqslant \frac{4L}{N_2} = 2\frac{E[D]}{(E[D])^2 + \mathrm{Var}[D]} < \frac{2}{E[D]}$$

In conclusion, there may exist a value ξ such that $\tau_c < \xi < \frac{2}{E[D]}$ for which $y_\infty(\xi) = \frac{1}{2}\frac{E[D]}{\lambda_1} < \frac{1}{2}$.

We end by deducing, approximately though, another type of lower bound. Concavity of $y_\infty(\tau)$ for $\tau \geqslant \tau_c = \frac{1}{\lambda_1}$ similarly leads to $y_\infty(q\tau_c + (1-q)m\tau_c) \geqslant (1-q)y_\infty(m\tau_c)$. For sufficiently large m, the Laurent series (23) up to first order leads to

$$y_\infty(m\tau_c) \geqslant 1 - \frac{1}{m\tau_c N}\sum_{j=1}^{N}\frac{1}{d_j}$$

because the second order term of $O\left(\frac{1}{(m\tau_c)^2}\right)$ is positive due to $\eta_2(i) > 0$ in (25). Choosing $q\tau_c + (1-q)m\tau_c = \frac{2}{E[D]}$ provides us with

$$y_\infty\left(\frac{2}{E[D]}\right) \geqslant \frac{\frac{2}{E[D]} - \tau_c}{(m-1)\tau_c}\left(1 - \frac{1}{m\tau_c N}\sum_{j=1}^{N}\frac{1}{d_j}\right) > \left(\frac{2\lambda_1}{E[D]} - 1\right)\frac{1}{m}\left(1 - \frac{\lambda_1 E\left[\frac{1}{D}\right]}{m}\right)$$

Ignoring the integer nature of m, the maximizer of the right-hand side occurs at $m = 2\lambda_1 E\left[\frac{1}{D}\right]$, resulting in

$$y_\infty\left(\frac{2}{E[D]}\right) \gtrapprox \frac{\frac{2\lambda_1}{E[D]} - 1}{4\lambda_1 E\left[\frac{1}{D}\right]}$$

Notice that $\frac{\frac{2\lambda_1}{E[D]}-1}{4\lambda_1 E\left[\frac{1}{D}\right]} \leqslant \frac{\frac{2\lambda_1}{E[D]}-1}{4\frac{\lambda_1}{E[D]}} < \frac{1}{2}$.

In summary, both last lower bound arguments illustrate, together with the upper bounds in Lemmas 6 and 7 that, for values of τ approaching $\frac{2}{E[D]}$, the steady-state fraction of infected nodes $y_\infty(\tau)$ is close to $\frac{1}{2}$ in any graph, in agreement with simulations [29].

8. Conclusion

We have reviewed and justified the viral conductance ψ as an additional virus-robustness metric to classify networks: the viral conductance ψ reflects the ease of virus spread in a network under all possible effective infection rates. In addition, we have derived easy to use analytic bounds on the viral conductance of different type: the general lower bounds (39) and (43) and upper bounds (40) and (42). Through a set of Lemmas 6–8, we have theoretically explained the observation that $y_\infty(s)$ is close to $\frac{1}{2}$ for $s = \frac{E[D]}{2}$, made by simulations in [29]. We show that the claim "among all graphs with N nodes and L links, the viral conductance is minimal for the regular graph" is correct, at least for the class of complete bipartite graphs. In a similar vein, we believe that the star has the largest viral conductance among all graphs with N nodes and L links. Rigorous proofs of both claims would be desirable. Finally, we have complemented the theory of N-intertwined model by deriving two series expansions (23) and (33) around $s = 0$ and $s = \lambda_1 = \frac{1}{\tau_c}$, respectively.

Two dynamic processes on graphs, virus spread and the coupling of oscillators, are argued to be mathematically related, which has inspired us to propose the synchronizability S as the analogue of the viral conductance ψ. An analysis as here still needs to be performed for the synchronizability, but we speculate that properties of ψ may translate to S for a same network.

Acknowledgement

We thank Mina Youssef and Caterina Scoglio for pointing us to the upper bound $\psi \leqslant \frac{\lambda_1}{2}$. This research was supported by Next Generation Infrastructures (Bsik) and the EU FP7 project ResumeNet (project No. 224619).

Appendix A. The continued fraction expansion

We present a slightly different derivation of the continued fraction in Theorem 9 proved in [27]:

Theorem 9. *For any effective spreading rate $\tau = \frac{\beta}{\delta} \geqslant 0$, the non-zero steady-state infection probability of any node i in the N-intertwined model can be expressed as a continued fraction*

$$v_{i\infty} = 1 - \cfrac{1}{1 + \tau d_i - \tau\sum_{j=1}^{N}\cfrac{a_{ij}}{1+\tau d_j - \tau\sum_{k=1}^{N}\cfrac{a_{jk}}{1+\tau d_k - \tau\sum_{q=1}^{N}\cfrac{a_{kq}}{1+\tau d_q - \ddots}}}} \tag{50}$$

where $d_i = \sum_{j=1}^{N} a_{ij}$ is the degree of node i.

Proof of Theorem 9. We rewrite (3) as

$$1 - v_{i\infty} = \frac{1}{1 + \tau d_i - \tau\sum_{j=1}^{N} a_{ij}(1 - v_{j\infty})}$$

and define the kth convergent as

$$w_i(k) = \frac{1}{1 + \tau d_i - \tau \sum_{j=1}^{N} a_{ij} w_j(k-1)} \tag{51}$$

with starting value $w_i(0) = 0$ and $v_{i\infty} = 1 - \lim_{k\to\infty} w_i(k)$. The difference $h_i(k) = w_i(k) - w_i(k-1)$, satisfying

$$h_i(k) = w_i(k) w_i(k-1) \tau \sum_{j=1}^{N} a_{ij} h_i(k-1)$$

with starting value $h_i(1) = (1+\tau d_i)^{-1}$, is bounded by

$$h_i(k) \geqslant \frac{\tau \sum_{j=1}^{N} a_{ij} h_i(k-1)}{(1+\tau d_i)^2} \geqslant 0$$

which shows that the sequence of convergents

$$w_i(0) \leqslant w_i(1) \leqslant \cdots \leqslant w_i(k-1) \leqslant w_i(k) \leqslant \cdots$$

is non-decreasing and leads, in the limit for $k \to \infty$, to the partial fraction (50). □

Appendix B

Proof of Lemma 5. After transforming (11) by $s = \frac{1}{\tau}$, differentiation with respect to s yields

$$\sum_{j=1}^{N} \frac{v_{j\infty}}{1 - v_{j\infty}} = \sum_{j=1}^{N} \left(d_j - \frac{s}{(1 - v_{j\infty})^2} \right) \frac{dv_{j\infty}}{ds}$$

Evaluation at the critical threshold $s = \lambda_1$, where $v_{j\infty} = 0$ for all $1 \leqslant j \leqslant N$ leads to

$$\sum_{j=1}^{N} d_j \frac{dv_{j\infty}}{ds} = \lambda_1 \sum_{j=1}^{N} \frac{dv_{j\infty}}{ds} = \lambda_1 N \frac{dy_\infty}{ds}\bigg|_{s=\lambda_1}$$

such that

$$\frac{dy_\infty}{ds}\bigg|_{s=\lambda_1} = \frac{1}{\lambda_1 N} \sum_{j=1}^{N} d_j \frac{dv_{j\infty}}{ds}\bigg|_{s=\lambda_1}$$

By definition of y_∞, we also have that

$$\frac{dy_\infty}{ds}\bigg|_{s=\lambda_1} = \frac{1}{N} \sum_{j=1}^{N} \frac{dv_{j\infty}}{ds}\bigg|_{s=\lambda_1} \tag{52}$$

Combining both yields, in vector notation,

$$\left(u - \frac{1}{\lambda_1} D \right)^T \frac{dV_\infty}{ds}\bigg|_{s=\lambda_1} = 0$$

This equality implies that the vector $\frac{dV_\infty}{ds}\big|_{s=\lambda_1}$ should be orthogonal to the vector $D - \lambda_1 u$. □

For a regular graph, $\frac{dv_{k\infty}}{ds} = -\frac{1}{d}$ and $D - \lambda_1 u = 0$. For any other non-regular graph, $d_{\max} > \lambda_1 > E[D]$ so that $D - \lambda_1 u$ has at least one positive component, while all components of $\frac{dV_\infty}{ds}\big|_{s=\lambda_1}$ are non-positive. Such condition on the vector components is necessary for orthogonality.

Appendix C

Proof of Lemma 2. By introduction of the Laurent series (23) into (3)

$$\left(1 + \tau \sum_{j=1}^{N} a_{ij} v_{j\infty} \right)$$

we obtain, with $\eta_0(i) = 1$,

$$\begin{aligned} 1 &= \left(1 - \sum_{j=0}^{\infty} \eta_j(i) \tau^{-j} \right) \left(1 + \tau \sum_{j=1}^{N} a_{ij} \sum_{k=0}^{\infty} \eta_k(j) \tau^{-k} \right) \\ &= 1 - \sum_{j=0}^{\infty} \eta_j(i) \tau^{-j} + \sum_{k=0}^{\infty} \sum_{j=1}^{N} a_{ij} \eta_k(j) \tau^{1-k} \\ &\quad - \sum_{m=0}^{\infty} \sum_{k=0}^{m} \left\{ \eta_{m-k}(i) \sum_{j=1}^{N} a_{ij} \eta_k(j) \right\} \tau^{1-m} \end{aligned}$$

Rewritten,

$$\begin{aligned} 0 &= -\sum_{m=0}^{\infty} \eta_m(i) \tau^{-m} + \sum_{m=0}^{\infty} \sum_{j=1}^{N} a_{ij} \eta_{m+1}(j) \tau^{-m} \\ &\quad - \sum_{m=0}^{\infty} \sum_{k=0}^{m+1} \left\{ \eta_{m+1-k}(i) \sum_{j=1}^{N} a_{ij} \eta_k(j) \right\} \tau^{-m} \end{aligned}$$

Equating corresponding powers in τ^{-m} yields, for $m \geqslant 0$

$$-\eta_m(i) + \sum_{j=1}^{N} a_{ij} \eta_{m+1}(j) - \sum_{k=0}^{m+1} \eta_{m+1-k}(i) \sum_{j=1}^{N} a_{ij} \eta_k(j) = 0$$

which is equivalent to

$$-\eta_m(i) - \sum_{k=0}^{m} \eta_{m+1-k}(i) \sum_{j=1}^{N} a_{ij} \eta_k(j) = 0$$

For $m = 0$ and $m = 1$, we find (24) and (25), while after rewriting the above relation, we arrive at the recursion (26) from which all powers can be determined in terms of the adjacency matrix elements. □

Appendix D. A power series expansion of $y_\infty(\tau)$ around $\tau_c^{-1} - \tau^{-1}$

Proof of Lemma 4. We substitute the definition (14) of V_∞ in terms of eigenvectors of the adjacency matrix A into the general steady-state Eq. (12), rewritten as

$$AV_\infty - \tau^{-1} V_\infty = \mathrm{diag}(v_{i\infty}) A V_\infty$$

and find

$$\sum_{k=1}^{N} (\lambda_k - \tau^{-1}) \gamma_k(\tau) x_k = \mathrm{diag}\left(\sum_{l=1}^{N} \gamma_l(\tau) (x_l)_i \right) \sum_{k=1}^{N} \gamma_k(\tau) \lambda_k x_k$$

After left-multiplication by x_m^T and exploiting the orthogonality between eigenvectors, we obtain

$$\begin{aligned} (\lambda_m - \tau^{-1}) \gamma_m(\tau) &= x_m^T \mathrm{diag}\left(\sum_{l=1}^{N} \gamma_l(\tau) (x_l)_i \right) \sum_{k=1}^{N} \gamma_k(\tau) \lambda_k x_k \\ &= \sum_{q=1}^{N} (x_m)_q \sum_{l=1}^{N} \gamma_l(\tau) (x_l)_q \sum_{k=1}^{N} \gamma_k(\tau) \lambda_k (x_k)_q \\ &= \sum_{l=1}^{N} \gamma_l(\tau) \sum_{k=1}^{N} \gamma_k(\tau) \lambda_k \sum_{q=1}^{N} (x_m)_q (x_l)_q (x_k)_q \end{aligned}$$

and

$$(\lambda_m - \tau^{-1})\gamma_m(\tau) = \sum_{l=1}^{N}\sum_{k=1}^{N}\gamma_l(\tau)\gamma_k(\tau)\lambda_k X(m,l,k) \quad (53)$$

where $X(m,l,k) = \sum_{q=1}^{N}(x_m)_q(x_l)_q(x_k)_q$ and $X(m,l,k)$ is unchanged by any permutation of the indices m, l and k. Introducing the power series (31) of $\gamma_k(\tau)$ into (53) and executing the Cauchy product for $\gamma_l(\tau)\gamma_k(\tau)$ yields

$$(\lambda_m - \tau^{-1})\sum_{j=0}^{\infty}c_j(m)(\tau_c^{-1} - \tau^{-1})^j = \sum_{j=0}^{\infty}\left\{\sum_{n=0}^{j}\sum_{l=1}^{N}\sum_{k=1}^{N}c_{j-n}(l)c_n(k)\lambda_k X(m,l,k)\right\}(\tau_c^{-1} - \tau^{-1})^j$$

Using $\tau_c^{-1} = \lambda_1$, the left-hand side is rewritten as

$$\begin{aligned}&(\lambda_m - \tau^{-1})\sum_{j=0}^{\infty}c_j(m)(\lambda_1 - \tau^{-1})^j\\ &= (\lambda_m - \lambda_1 + \lambda_1 - \tau^{-1})\sum_{j=0}^{\infty}c_j(m)(\lambda_1 - \tau^{-1})^j\\ &= (\lambda_m - \lambda_1)\sum_{j=0}^{\infty}c_j(m)(\lambda_1 - \tau^{-1})^j + \sum_{j=0}^{\infty}c_j(m)(\lambda_1 - \tau^{-1})^{j+1}\\ &= \sum_{j=0}^{\infty}(\lambda_m - \lambda_1)c_j(m)(\lambda_1 - \tau^{-1})^j + \sum_{j=1}^{\infty}c_{j-1}(m)(\lambda_1 - \tau^{-1})^j\end{aligned}$$

Equating corresponding powers in $(\lambda_1 - \tau^{-1})^j$ yields, for $j = 0$,

$$(\lambda_m - \lambda_1)c_0(m) = \sum_{l=1}^{N}\sum_{k=1}^{N}c_0(l)c_0(k)\lambda_k X(m,l,k) = 0$$

because $c_0(k) = 0$ for all $1 \leqslant k \leqslant N$ and, for $j > 0$,

$$\begin{aligned}(\lambda_m - \lambda_1)c_j(m) + c_{j-1}(m) &= \sum_{n=0}^{j}\sum_{l=1}^{N}\sum_{k=1}^{N}c_{j-n}(l)c_n(k)\lambda_k X(m,l,k)\\ &= \sum_{n=1}^{j-1}\sum_{l=1}^{N}\sum_{k=1}^{N}c_{j-n}(l)c_n(k)\lambda_k X(m,l,k)\end{aligned}$$

Before proceeding, we confine to the case where $j = 1$, $(\lambda_m - \lambda_1)c_1(m) = 0$, illustrating that all $c_1(m) = 0$ for $m > 1$, except when $m = 1$, which is in agreement with Theorem 3. Next, the case for $j = 2$ yields

$$\begin{aligned}(\lambda_m - \lambda_1)c_2(m) + c_1(m) &= \sum_{l=1}^{N}\sum_{k=1}^{N}c_1(l)c_1(k)\lambda_k X(m,l,k)\\ &= c_1^2(1)\lambda_1 X(m,1,1)\end{aligned}$$

so that, for $m = 1$, taking into account that $c_1(m) = 0$ for $m > 1$, $c_1(1) = c_1^2(1)\lambda_1 X(1,1,1)$

or $c_1(1) = (\lambda_1 X(1,1,1))^{-1}$, which is also in agreement with Theorem 3, while for $m > 1$, we obtain

$$c_2(m) = -\frac{c_1^2(1)}{\lambda_1 - \lambda_m}\lambda_1 X(m,1,1) = -\frac{1}{\lambda_1 - \lambda_m}\frac{X(m,1,1)}{\lambda_1 X^2(1,1,1)}$$

Continuing, for $j > 2$ and using that all $c_1(m) = 0$ for $2 \leqslant m \leqslant N$, except for $c_1(1)$, we have

$$\begin{aligned}&(\lambda_m - \lambda_1)c_j(m) + c_{j-1}(m)\\ &= \sum_{l=1}^{N}\sum_{k=1}^{N}c_{j-1}(l)c_1(k)\lambda_k X(m,l,k) + \sum_{l=1}^{N}\sum_{k=1}^{N}c_1(l)c_{j-1}(k)\lambda_k X(m,l,k)\\ &\quad + \sum_{n=2}^{j-2}\sum_{l=1}^{N}\sum_{k=1}^{N}c_{j-n}(l)c_n(k)\lambda_k X(m,l,k)\\ &= c_1(1)\lambda_1\sum_{l=1}^{N}c_{j-1}(l)X(m,l,1) + c_1(1)\sum_{k=1}^{N}c_{j-1}(k)\lambda_k X(m,1,k)\\ &\quad + \sum_{n=2}^{j-2}\sum_{l=1}^{N}\sum_{k=1}^{N}c_{j-n}(l)c_n(k)\lambda_k X(m,l,k)\end{aligned}$$

Permutation of the indices leaves $X(m,l,k)$ unchanged,

$$\begin{aligned}&c_1(1)\lambda_1\sum_{l=1}^{N}c_{j-1}(l)X(m,l,1) + c_1(1)\sum_{k=1}^{N}c_{j-1}(k)\lambda_k X(m,1,k)\\ &= c_1(1)\sum_{k=1}^{N}(\lambda_1 + \lambda_k)c_{j-1}(k)X(m,k,1)\end{aligned}$$

leading to

$$\begin{aligned}&(\lambda_m - \lambda_1)c_j(m) + c_{j-1}(m)\\ &= c_1(1)\sum_{k=1}^{N}(\lambda_1 + \lambda_k)c_{j-1}(k)X(m,k,1)\\ &\quad + \sum_{n=2}^{j-2}\sum_{l=1}^{N}\sum_{k=1}^{N}c_{j-n}(l)c_n(k)\lambda_k X(m,l,k)\\ &= c_1(1)(\lambda_1 + \lambda_m)c_{j-1}(m)X(m,m,1)\\ &\quad + c_1(1)\sum_{k=1;k\neq m}^{N}(\lambda_1 + \lambda_k)c_{j-1}(k)X(m,k,1)\\ &\quad + \sum_{n=2}^{j-2}\sum_{l=1}^{N}\sum_{k=1}^{N}c_{j-n}(l)c_n(k)\lambda_k X(m,l,k)\end{aligned}$$

Finally, after rearrangement, we arrive at the general recursion (34) for the coefficients $c_j(m)$ for $m > 1$ and $j > 2$. The recursion for $c_j(1)$ and $j > 2$ follows as

$$\begin{aligned}c_{j-1}(1) &= \frac{c_1(1)\sum_{k=2}^{N}(\lambda_1 + \lambda_k)c_{j-1}(k)X(1,1,k)}{1 - 2c_1(1)\lambda_1 X(1,1,1)}\\ &\quad + \frac{\sum_{n=2}^{j-2}\sum_{l=1}^{N}\sum_{k=1}^{N}c_{j-n}(l)c_n(k)\lambda_k X(1,l,k)}{1 - 2c_1(1)\lambda_1 X(1,1,1)}\end{aligned}$$

With $c_1(1) = (\lambda_1 X(1,1,1))^{-1}$, we arrive at (36). This proves Lemma 4. □

For example, for $j = 2$ in (36),

$$c_2(1) = -\frac{1}{\lambda_1 X(1,1,1)}\sum_{k=2}^{N}(\lambda_1 + \lambda_k)c_2(k)X(1,1,k)$$

Using (35),

$$c_2(1) = \frac{1}{\lambda_1^2 X^3(1,1,1)}\sum_{k=2}^{N}\frac{\lambda_1 + \lambda_k}{\lambda_1 - \lambda_k}X^2(k,1,1) \quad (54)$$

After the transformation $s = \frac{1}{\tau}$, the derivatives

$$\left.\frac{d^j y_\infty(s)}{ds^j}\right|_{s\uparrow\lambda_1} = \frac{j!}{N}\sum_{k=1}^{N}c_j(k)u^T x_k$$

are immediate from (32). In particular, for $j = 2$, we obtain

$$\left.\frac{d^2 y_\infty(s)}{ds^2}\right|_{s=\lambda_1} = \frac{2}{N}c_2(1)u^T x_1 + \frac{2}{N}\sum_{k=2}^{N}c_2(k)u^T x_k$$

and substituting (54) and (35) yields

$$\begin{aligned}\left.\frac{d^2 y_\infty(s)}{ds^2}\right|_{s\uparrow\lambda_1} &= \frac{2u^T x_1}{N\lambda_1^2 X^3(1,1,1)}\sum_{k=2}^{N}\frac{\lambda_1 + \lambda_k}{\lambda_1 - \lambda_k}X^2(k,1,1)\\ &\quad - \frac{2}{N\lambda_1 X^2(1,1,1)}\sum_{k=2}^{N}\frac{u^T x_k}{\lambda_1 - \lambda_k}X(k,1,1) \quad (55)\end{aligned}$$

For example, from (20), the second derivative at $s \to \lambda_1 = \sqrt{mn}$ for the complete bi-partite graph is

$$\left.\frac{d^2y_\infty(s)}{ds^2}\right|_{s\uparrow\lambda_1} = \frac{2}{N\sqrt{mn}}\left(\frac{\sqrt{m}-\sqrt{n}}{\sqrt{m}+\sqrt{n}}\right)^2$$

The general formula (55) requires the determination of $X(k,1,1)$. With $x_1^T = \left[\frac{u_{1\times m}}{\sqrt{2m}} \quad \frac{u_{1\times n}}{\sqrt{2n}}\right]$, we have

$$X(k,1,1) = \sum_{q=1}^{N}(x_k)_q(x_1)_q^2 = \frac{1}{2m}\sum_{q=1}^{m}(x_k)_q + \frac{1}{2n}\sum_{q=m+1}^{N}(x_k)_q$$

Orthogonality of x_k and x_1 implies that

$$0 = \sum_{q=1}^{N}(x_k)_q(x_1)_q = \frac{1}{\sqrt{2m}}\sum_{q=1}^{m}(x_k)_q + \frac{1}{\sqrt{2n}}\sum_{q=m+1}^{N}(x_k)_q$$

and, similarly, orthogonality of x_k and $x_N = \left[\frac{u_{1\times m}}{\sqrt{2m}} \quad -\frac{u_{1\times n}}{\sqrt{2n}}\right]^T$ results in

$$0 = \sum_{q=1}^{N}(x_k)_q(x_N)_q = \frac{1}{\sqrt{2m}}\sum_{q=1}^{m}(x_k)_q - \frac{1}{\sqrt{2n}}\sum_{q=m+1}^{N}(x_k)_q$$

Hence, for $1 < k < N$, we have that $\sum_{q=1}^{m}(x_k)_q = 0$ and $\sum_{q=m+1}^{N}(x_k)_q = 0$ so that $X(k,1,1) = 0$. With $\lambda_N = -\lambda_1 = \sqrt{nm}$ and

$$X(N,1,1) = \frac{1}{2\sqrt{2}}\left(\frac{1}{\sqrt{m}} - \frac{1}{\sqrt{n}}\right)$$
$$X(1,1,1) = \frac{1}{2\sqrt{2}}\left(\frac{1}{\sqrt{m}} + \frac{1}{\sqrt{n}}\right)$$

we obtain from (55)

$$\left.\frac{d^2y_\infty(s)}{ds^2}\right|_{s\uparrow\lambda_1} = -\frac{2}{N\lambda_1 X^2(1,1,1)}\frac{u^T x_N}{\lambda_1-\lambda_N}X(N,1,1) = \frac{2}{N\sqrt{mn}}\left(\frac{\sqrt{m}-\sqrt{n}}{\sqrt{m}+\sqrt{n}}\right)^2$$

which agrees with direct derivation of the closed form (20). □

Appendix E

Proof of Lemma 1. The viral conductance (20) of the bipartite graph $K_{n,m}$ is, with $E[D] = \frac{2nm}{N}$,

$$\psi_{K_{n,m}} = \frac{E[D]}{2} + Y_{n,m}$$

where

$$Y_{n,m} = \sqrt{mn} - \frac{2mn}{N} + \frac{(n-m)}{N}\log\frac{\left(1+\sqrt{\frac{n}{m}}\right)^m}{\left(1+\sqrt{\frac{m}{n}}\right)^n}$$

and we need to show that $Y_{n,m}$ is always positive for $n > m$ and only zero if $n = m$. First, with

$$\sqrt{mn} - \frac{2mn}{N} = \frac{\sqrt{mn}}{N}\left(m+n-2\sqrt{mn}\right) = \frac{\sqrt{mn}}{N}\left(\sqrt{m}-\sqrt{n}\right)^2$$

we have

$$NY_{n,m} = \sqrt{mn}\left(\sqrt{n}-\sqrt{m}\right)^2 + (n-m)\log\frac{\left(1+\sqrt{\frac{n}{m}}\right)^m}{\left(1+\sqrt{\frac{m}{n}}\right)^n}$$

which shows that $Y_{n,m} = 0$ for $n = m$. In addition, symmetry applies so that $NY_{n,m} = NY_{m,n}$ which allows us to further confine to the case that $n > m$. Next, assuming that $n > m$, we rewrite

$$\log\frac{\left(1+\sqrt{\frac{n}{m}}\right)^m}{\left(1+\sqrt{\frac{m}{n}}\right)^n} = \frac{m}{2}\log\left(\frac{n}{m}\right) - (n-m)\log\left(1+\sqrt{\frac{m}{n}}\right)$$

so that

$$NY_{n,m} = \sqrt{mn}\left(\sqrt{n}-\sqrt{m}\right)^2 + (n-m)\frac{m}{2}\log\left(\frac{n}{m}\right) - (n-m)^2 \times \log\left(1+\sqrt{\frac{m}{n}}\right) \tag{56}$$

and

$$\frac{NY_{n,m}}{(n-m)^2} = \frac{\sqrt{mn}}{\left(\sqrt{n}+\sqrt{m}\right)^2} + \frac{m}{2(n-m)}\log\left(\frac{n}{m}\right) - \log\left(1+\sqrt{\frac{m}{n}}\right) = \frac{\sqrt{\frac{n}{m}}}{\left(1+\sqrt{\frac{n}{m}}\right)^2} - \frac{\frac{m}{n}}{2\left(1-\frac{m}{n}\right)}\log\left(\frac{m}{n}\right) - \log\left(1+\sqrt{\frac{m}{n}}\right)$$

With $y = \frac{m}{n} \in [0,1]$, we have

$$\frac{NY_{n,m}}{(n-m)^2} = g(y) = \frac{\sqrt{y}}{\left(1+\sqrt{y}\right)^2} - \frac{y}{2(1-y)}\log(y) - \log\left(1+\sqrt{y}\right)$$

where $g(0) = 0$. The function $g(y)$ is monotonous increasing for $0 \leqslant y \leqslant 1$ because $g'(y) = \frac{-4(1-\sqrt{y})-(1+\sqrt{y})\log y}{2(1-\sqrt{y})^2(1+\sqrt{y})}$ and $-(1+\sqrt{y})\log y > 4(1-\sqrt{y})$. The latter inequality follows from the expansion $\log z = -2\sum_{k=1}^{\infty}\frac{1}{2k-1}\left(\frac{1-z}{1+z}\right)^{2k-1}$, valid for $\mathrm{Re}(z) \geqslant 0$, but $z \neq 0$ (see [1, Section 4.1.27]), for $z = \sqrt{y}$. Hence, for $0 \leqslant y \leqslant 1$, $g'(y) \geqslant 0$ so that $g(y) \geqslant 0$ and this proves Lemma 1. □

References

[1] M. Abramowitz, I.A. Stegun, Handbook of Mathematical Functions, Dover Publications, Inc., New York, 1968.
[2] R.M. Anderson, R.M. May, Infectious Diseases of Humans: Dynamics and Control, Oxford University Press, Oxford, UK, 1991.
[3] A. Barrat, M. Bartelemy, A. Vespignani, Dynamical Processes on Complex Networks, Cambridge University Press, Cambridge, U.K., 2008.
[4] C. Castellano, R. Pastor-Satorras, Thresholds for epidemic spreading in networks, Physical Review Letters 105 (2010) 218701. November.
[5] E. Cator, P. Van Mieghem, Second-order mean-field susceptible-infected-susceptible epidemic threshold, Physical Review E 85 (5) (2012) 056111.
[6] D. Chakrabarti, Y. Wang, C. Wang, J. Leskovec, C. Faloutsos, Epidemic thresholds in real networks, ACM Transactions on Information and System Security (TISSEC) 10 (4) (2008) 1–26.
[7] F. Darabi Sahneh, C. Scoglio, Epidemic spread in human networks, in: 50th IEEE Conference on Decision and Control, Orlando, FL, USA, December 2011. Available from: arXiv:1107.2464v1.
[8] M. Draief, L. Massoulié, Epidemics and Rumours in Complex Networks, London Mathematical Society Lecture Node Series, 369, Cambridge University Press, Cambridge, UK, 2010.
[9] A. Ganesh, L. Massoulié, D. Towsley, The effect of network topology on the spread of epidemics, IEEE INFOCOM05 (2005).
[10] E. Gourdin, J. Omic, P. Van Mieghem, Optimization of network protection against virus spread, in: 8th International Workshop on Design of Reliable Communication Networks (DRCN 2011), Krakow, Poland, October 10–12, 2011.
[11] R.E. Kooij, P. Schumm, C. Scoglio, M. Youssef. A new metric for robustness with respect to virus spread, Networking 2009, LNCS 5550, 2009, pp. 562–572.
[12] C. Li, R. van de Bovenkamp, P. Van Mieghem, The SIS mean-field N-intertwined and Vespignani approximation: a comparison, Physical Review E, accepted for publication.
[13] C. Li, H. Wang, W. de Haan, C.J. Stam, P. Van Mieghem, The correlation of metrics in complex networks with applications in functional brain networks, Journal of Statistical Mechanics: Theory and Experiment (JSTAT) (2011) P11018. November.
[14] J. Omic, Epidemics in networks: modeling, optimization and security games, Delft University of Technology, Ph.D. Thesis, September 2010. <http://repository.tudelft.nl/>.
[15] J. Omic, P. Van Mieghem, Epidemic spreading in networks – variance of the number of infected nodes, Delft University of Technology, Report20090707, 2009. <www.nas.ewi.tudelft.nl/people/Piet/TUDelftReports>.
[16] R. Pastor-Satorras, A. Vespignani, Epidemic dynamics and endemic states in complex networks, Physical Review E 63 (2001) 066117.
[17] J.G. Restrepo, E. Ott, Brian R. Hunt, Onset of synchronization in large networks of coupled oscillators, Physical Review E 71 (036151) (2005) 1–12.
[18] F.D. Sahneh, C. Scoglio, and P. Van Mieghem. Generalized epidemic mean-field model for spreading processes over multi-layer complex networks, accepted for publication.

[19] S.H. Strogatz, From Kuramoto to Crawford: exploring the onset of synchronization in populations of coupled oscillators, Physica D 143 (2000) 1–20.
[20] S. Tang, N. Blenn, C. Doerr, P. Van Mieghem, Digging in the digg online social network, IEEE Transactions on Multimedia 13 (5) (2011) 1163–1175. October.
[21] P. Van Mieghem, Performance Analysis of Communications Systems Networks, Cambridge University Press, Cambridge, U.K., 2006.
[22] P. Van Mieghem, Graph Spectra for Complex Networks, Cambridge University Press, Cambridge, U.K., 2011.
[23] P. Van Mieghem, The *N*-Intertwined SIS epidemic network model, Computing 93 (2) (2011) 147–169.
[24] P. Van Mieghem, Epidemic phase transition of the SIS-type in networks, Europhysics Letters (EPL) 97 (2012) 48004.
[25] P. Van Mieghem, C. Doerr, H. Wang, J. Martin Hernandez, D. Hutchison, M. Karaliopoulos, R.E. Kooij, A framework for computing topological network robustness, Delft University of Technology, Report20101218, 2010. <www.nas.ewi.tudelft.nl/people/Piet/TUDelftReports>.
[26] P. Van Mieghem, J. Omic, In-homogeneous virus spread in networks, Delft University of Technology, Report2008081, 2008. <www.nas.ewi.tudelft.nl/people/Piet/TUDelftReports>.
[27] P. Van Mieghem, J. Omic, R.E. Kooij, Virus spread in networks, IEEE/ACM Transactions on Networking 17 (1) (2009) 1–14. February.
[28] Y. Wang, D. Chakrabarti, C. Wang, C. Faloutsos. Epidemic spreading in real networks: An eigenvalue viewpoint, in: 22nd International Symposium on Reliable Distributed Systems (SRDS'03), IEEE Computer, October 2003, pp. 25–34.
[29] M. Youssef, R.E. Kooij, C. Scoglio, Viral conductance Quantifying the robustness of networks with respect to spread of epidemics, Journal of Computational Science (2011), http://dx.doi.org/10.1016/j.jocs.2011.03.001.
[30] M. Youssef, C. Scoglio, An individual-based approach to SIR epidemics in contact networks, Journal of Theoretical Biology 283: (2011) 136–144.